JCTC Journal of Chemical Theory and Computation

ARTICLE

pubs.acs.org/JCTC

An Integrated Protocol for the Accurate Calculation of Magnetic Interactions in Organic Magnets

Vincenzo Barone,[†] Ivo Cacelli,[‡] Alessandro Ferretti,[§] Susanna Monti,[§] and Giacomo Prampolini*[,†]

[†]Scuola Normale Superiore, piazza dei Cavalieri 7, I-56126 Pisa, Italy

[‡]Dipartimento di Chimica e Chimica Industriale, Università degli Studi di Pisa, via Risorgimento 35, I-56126 Pisa, Italy

[§]Istituto di Chimica dei Composti OrganoMetallici (ICCOM-CNR), Area della Ricerca, via G. Moruzzi 1, I-56124 Pisa, Italy

ABSTRACT: A new, fast, and efficient computational protocol for the accurate calculation of singlet−triplet magnetic splittings in organic diradicals is tested and validated. This procedure essentially consists of three steps: the adoption of modified virtual orbitals (MVO) and a mixed variational−perturbational approach (CSPA) are now combined with a third method that exploits the reduction of the configurational space dimensions achieved by fragmentation/localization criteria. This innovative approach is successfully tested on four different substituted *m*-phenylene bis(*tert*-butyl) nitroxides, which show paramagnetic behavior, by computing singlet−triplet energy gaps and comparing them with their experimental counterparts.

1. INTRODUCTION

The multidisciplinary interest in organic di- and poliradicals[1−7] stems from the many technological applications in which they are involved, ranging from spintronics (as sensing, memory, or switching devices[1,2,8−12]) to soft matter (as contrast agents for magnetic resonance imaging, spin labels, or mediators for controlled radical polymerization[13−16]). Among diradicals, many substituted *m*-phenylene-bridged nitroxides have been synthesized and proposed as stable paramagnetic materials by several groups.[12,16−23] Besides being prototypes of organic paramagnetic compounds, these species may be important as basic units of polyradical systems,[16,17,23] thus being potentially appealing in the design of magnetic devices or biologically relevant probes. A key feature in molecular magnetism is clearly the singlet−triplet energy gap, ΔE_{ST}. This quantity is not directly accessible by experiments, but it can be derived through a numerical fit[12,16,17,19−24] from the temperature dependence of the magnetic susceptibility (χ) obtained by superconducting quantum interference device (SQUID) magnetometry. Unfortunately, at variance with antiferromagnetic interactions, the sensitivity of this method to the values of ΔE_{ST} for ferromagnetic materials in solution is rather small[1,18,22,24] and often allows only for a determination of a lower limit of ΔE_{ST},[22,24] rather than its actual value.

From a computational point of view, the calculation of ΔE_{ST} is also challenging, due to the difficulties in defining a protocol possessing at the same time the required characteristics of accuracy and feasibility. Furthermore, in diradicals where the magnetic moieties are bridged by an unsaturated fragment, the coupling between the spins of the two unpaired electrons is strongly affected by the presence of the bridge itself, and any attempt to calculate ΔE_{ST} should take into account its presence explicitly. On the one hand, computational convenience would suggest resorting to Density Functional Theory (DFT), adopting the Noodleman broken-symmetry method[25,26] to calculate the magnetic splitting. This method, widely applied to inorganic and organic species,[27−33] has been recently reviewed by several authors.[33−35] However, its theoretical foundation and robustness are rather questionable. On the other hand, the more rigorous post-Hartree−Fock methods[36−54] become rapidly unfeasible with the increase of the molecular dimensions. Although computational feasibility would suggest employing second order perturbation methods, the neglect of the interaction terms between the perturbers invalidates the accuracy of the results and makes variational approaches much more reliable. Among these, the Difference Dedicated Configuration Interaction methods (DDCI and DDCI2)[37,38,42] allow for a remarkable reduction of the full CI space dimensions. Indeed, the DDCI2 scheme[42] is certainly less expensive, and it was recently shown to yield reliable results for small organic diradicals.[55,56] Nonetheless, some inaccuracies were reported in other cases,[57] where better performances were obtained, for paramagnetic molecules, with the adoption of the complete DDCI approach. However, the dimensions of the DDCI configurational space increase very rapidly with the molecular size, and the direct application of the DDCI scheme to large molecules remains unfeasible.

To circumvent this problem, a multilevel strategy has been recently[56,58,59] developed in our group. The new methodology allows us to sensibly reduce the dimensions of the DDCI space with a negligible loss of accuracy. Essentially, the approach consists of three different steps. First, molecular orbitals are localized onto different moieties, and those belonging to the fragments outside the magnetic+bridge moiety are neglected.[56] In a second step, computational advantages can also be obtained by the use of modified virtual orbitals (MVOs), built adding extra charges to the magnetic sites.[58] Indeed, the size of the DDCI space can be further reduced by neglecting excitations to high energy virtual orbitals, and it has been shown[58] that faster convergence can be achieved if the virtual orbitals to be excluded are chosen among the modified rather than the canonical ones. Finally, the use of the Complementary Space Perturbative Approach (CSPA)[59] allows for a further reduction of the dimensions of the variational DDCI configurational space. In fact, only a small fraction of the

Received: October 21, 2010
Published: January 19, 2011

Table 1. Configurational Classes Considered within the DDCI Scheme[a]

class	description	class[42]
N.2.0	the primary four-dimensional space (includes kinetic exchange)	
N.1.1	single excitations from magnetic orbitals	1p
N.0.2	double excitations from magnetic orbitals	2p
N-1.3.0	single excitations from core to magnetic orbitals (related to superexchange)	1h
N-1.2.1	single excitations from core to unoccupied orbitals (include spin polarization)	1h + 1p
N-2.4.2	double excitations from core to magnetic orbitals	2h
N-1.1.2	simultaneous excitations from core and magnetic to unoccupied orbitals	1h + 2p
N-2.3.1	double excitations from core to magnetic and unoccupied orbitals	2h + 1p

[a] Each class is labeled in terms of three numbers (first column) referring to core, magnetic, and unoccupied molecular orbitals. In the last column, the corresponding notation proposed by Calzado et al.[42] is reported. The configurational classes reported in the last two rows are not included in a DDCI2 scheme.

MVOs is considered in the variational treatment, whereas the remaining part is handled through a Möller−Plesset perturbative approach. This protocol, recently tested on a diaryl-nitroxide diradical,[22,60] is here proposed and validated for a series of four substituted *m*-phenylene-bridged *tert*-butyl-nitroxides.[12,16,17,21]

The paper is organized as follows: in the next section, employed methods are briefly reviewed and computational details are given. Results are presented and discussed in section 3, while main conclusions are drawn in the last section.

2. METHODS AND COMPUTATIONAL DETAILS

2.1. Methods. *2.1.1. DDCI.* The minimal description of magnetic interactions in a diradical system can be given within the four-dimensional configurational space obtained placing the two unpaired electrons in two nearly degenerate molecular orbitals (MOs) $|\phi_g\rangle$ and $|\phi_u\rangle$. To obtain a more transparent physical description, one may localize the canonical MOs through a unitary transformation into orbitals $|\phi_a\rangle$ and $|\phi_b\rangle$, which can in turn be used to generate the four basic configurations:

$$
\begin{aligned}
|^1\Psi_A\rangle &= \frac{1}{\sqrt{2}}(|...\phi_a\overline{\phi}_b\rangle + |...\phi_b\overline{\phi}_a\rangle)\\
|^1\Psi_B\rangle &= |...\phi_a\overline{\phi}_a\rangle\\
|^1\Psi_C\rangle &= |...\phi_b\overline{\phi}_b\rangle\\
|^3\Psi\rangle &= \frac{1}{\sqrt{2}}(|...\phi_a\overline{\phi}_b\rangle - |...\phi_b\overline{\phi}_a\rangle)
\end{aligned}
\qquad (1)
$$

Among the resulting states, $|^1\Psi_A\rangle$ and $|^3\Psi\rangle$ provide the main contribution to the singlet−triplet energy gap in weakly coupled diradicals, since the ionic configurations ($|^1\Psi_B\rangle$ and $|^1\Psi_C\rangle$) lie at higher energies. Clearly, this basic configurational space alone is insufficient to provide a reliable estimate of the ΔE_{ST} ($E_S - E_T$) gap, and other classes of configurations should be considered. In the DDCI and DDCI2[37,38,42] approaches, only those classes that are expected to give a non-negligible contribution to ΔE_{ST} are selected and employed during the calculation. Thus, besides the four configurations reported in eq 1, DDCI includes all determinants arising from single and double excitations from the magnetic to the virtual orbitals, together with double excitations from the magnetic and core orbitals to the virtual orbitals, but involving one single core-to-virtual excitation. All of these classes are reported in Table 1, where differences between the DDCI and DDCI2 approaches are underlined in the last two rows. Further details can be found in refs 56 and 58−60 and references therein.

2.1.2. Three-Step Procedure. Despite this selection, the size of DDCI configurational space increases still rapidly with the molecular dimensions, making a full variational approach with the standard DDCI scheme unfeasible for large molecules. The first step of the proposed protocol is based on fragment localization (step I): MOs are first localized onto specific moieties through the Pipek−Mezey method,[61] and only those belonging to the fragments involved in the magnetic interaction (magnetic+bridge moieties) are retained for the DCCI calculation.[55,56]

Once the virtual orbitals (VOs) localized on the "external" fragments have been removed, the Modified Virtual Orbital (MVO) scheme[58] is applied (step II) on the remaining VOs space. MVOs are determined by the following eigenvalue equation:

$$(\hat{F} + \hat{V})\phi_\mu = \epsilon_\mu\phi_\mu \qquad (2)$$

where $\hat{F}$ is the Fock operator for the restricted triplet state and $\hat{V}$ is a supplementary nuclear potential obtained placing some extra charges q_α at the positions R_α, i.e.,

$$\hat{V} = -\sum_\alpha \frac{q_\alpha}{|R_\alpha - r|}$$

where the summation is restricted to those atoms bearing the magnetic orbitals. The effective optimal supplementary charges were determined in previous work,[58,59] on the basis of the convergence properties of the resulting MVOs in the DDCI2 or DDCI scheme, resulting in $q_\alpha = 1$ or 2, respectively. More details about the method can be found in the original paper.[58] Here, it is worth highlighting that the computed MVOs allow significant advantages, in that those having the lowest ε_μ's (see eq 2) are the most involved in the spin−spin coupling, whereas decreasing effects are observed with the increase of the orbital energy.

Finally, in step III, the CSPA approach[59] is applied. In the hypothesis that the interaction terms between the perturbers play a major role in ΔE_{ST} only for those configurations which involve excitations to the lowest MVOs, the variational calculation is performed only for a fraction of MVOs, while the rest of the configurations is handled by a multireference perturbative treatment, using the so-called barycentric Möller−Plesset partition. In this way, only a small portion of the MVOs (i.e., those at low energy, thus more involved in the magnetic coupling) is active for the variational calculation, but all of them are considered for the (cheaper) perturbative calculation. A pictorial representation of steps I−III is sketched in Figure 1.

2.2. Computational Details. All molecular structures have been optimized in their triplet state at the DFT-UB3LYP/cc-pvdz

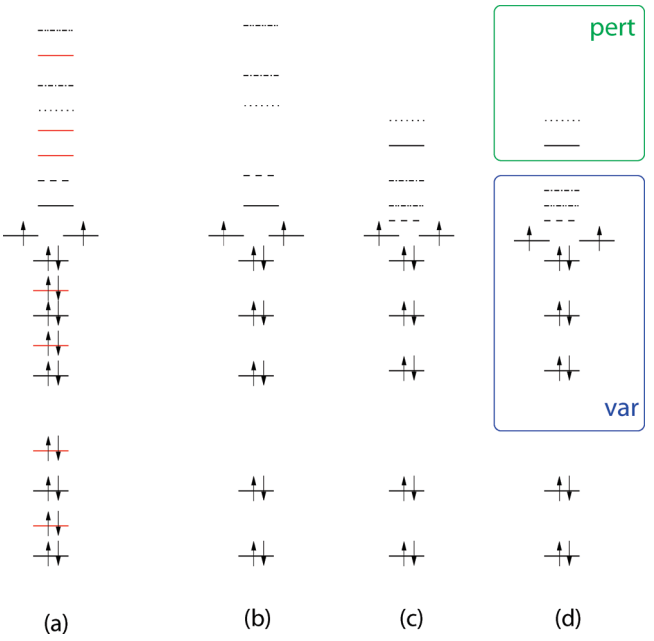

Figure 1. Scheme of the multilevel protocol. (a) All MOs are first localized into active (black) and external (red) fragments. (b) Step I: MOs on external fragments are excluded from DDCI calculations. (c) Step II: VOs are modified through MVO approach. (d) Step III: Only a fraction of orbitals is treated variationally (blue window), while other MVOs (green window) are taken into account through a perturbative approach (CSPA) .

level of theory using the Gaussian package.[62] Unless otherwise stated, all torsional potential energy surfaces have been computed by optimizing all geometries with no symmetry restrictions but the investigated torsional angles. The canonical molecular orbitals were obtained by a ROHF calculation for the triplet state, using the GAMESS code,[63] with the 6-31G(d) basis set. The MVOs were obtained using the Fortran program QUIOLA coded by the authors, which interfaces the GAMESS output files with the routine for the transformation of the integrals from the atomic to the molecular basis set.[55] The CI calculations were performed using the CIPSI program,[64−66] which has been rewritten[59] in order to improve efficiency and to manage the CSPA calculations. In all CI calculations, all 1s core orbitals were always kept inactive with occupation number 2 in all configurations.

3. RESULTS AND DISCUSSION

The singlet−triplet energy gap ΔE_{ST} was computed for a group of substituted *m*-phenylene bis(*tert*-butylnitroxide) diradicals, namely, *m*-phenylene bis(*tert*-butyl) nitroxide[17] (compound **1**), 4,6-bis(trifluoromethyl)-N,NA-di-*tert*-butyl-1,3-phenylenebis-(aminoxyl)[21] (**2**), biphenyl-3,5-diyl bis(*tert*-butyl-nitroxide)[12,19,20] (**3**), and a polyethylene glycol (PEG) functionalized (pegylated) bis(aminoxyl) diradical[16] (**4**), whose structures and measured singlet−triplet energy gaps are reported in Figure 2 and in Table 2, respectively. Besides testing the proposed integrated strategy, our aim is also to investigate the contributions to ΔE_{ST} of the different substituents. The following discussion has been thus separated for each of the considered species.

3.1. *m*-Phenylene Bis(*tert*-butyl) Nitroxide. Diradical **1** is the smallest prototype of *m*-phenylene bis(*tert*-butyl nitroxide) diradicals, thus constituting an ideal candidate to test and validate

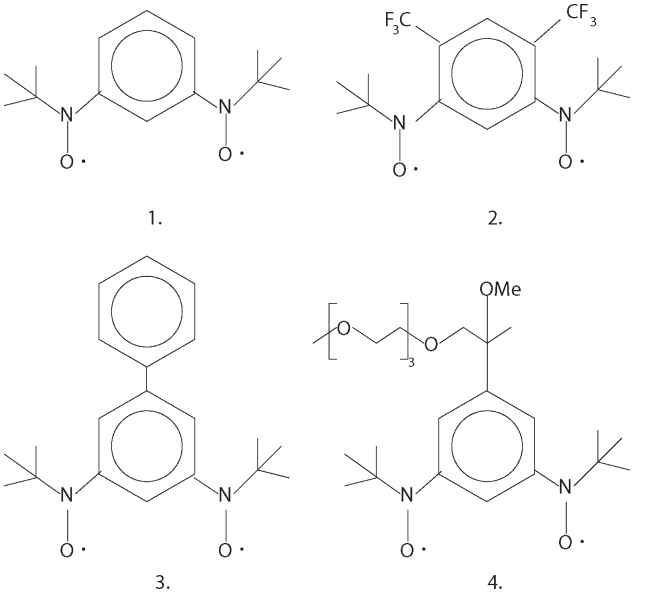

Figure 2. Substituted nitroxide diradicals studied in the present work. (**1**) *m*-Phenylene bis(*tert*-butyl nitroxide);[17] (**2**) 4,6-bis(trifluoromethyl)-N,NA-di-*tert*-butyl-1,3-phenylene bis(aminoxyl); (**3**) biphenyl-3,5-diyl bis(*tert*-butyl nitroxide);[12,19,20] (**4**) pegylated bis(aminoxyl) diradical.[16]

Table 2. Experimental Estimates of the Singlet−Triplet Energy Gap ΔE_{ST}, As Obtained from the Best Fit Theoretical Curves of SQUID Data for Compounds 1−4 of Figure 2

diradical	ΔE_{ST} (K)	ΔE_{ST} (cm^{-1})	ref
1	>300	>210	17
2	∼80	∼55	21
3	>350	>241	20
4	∼650	∼450	16

the computational procedure proposed in the present work. In fact, despite its dimensions not allowing a complete DDCI variational treatment, diradical **1** can be handled within the CSPA approach without resorting to fragmentation schemes. In particular, in view of the calculations to be performed on the next larger compounds, it could be computationally advantageous to substitute the *tert*-butyl moieties with methyl groups, in the hypothesis that their contribution to ΔE_{ST} can be neglected. With this aim, a *m*-phenylene bis(methyl nitroxide) diradical was optimized in two different geometries (see Figure 3). In the first case (**1a**), a full optimization was performed directly on the small methyl-nitroxide diradical, whereas the second geometry (**1b**) was obtained by substituting a hydrogen atom with each of the three methyl groups of a fully optimized geometry of the whole diradical **1**. In the latter case, only the hydrogen atoms were reoptimized after substitution. Clearly, the former route is less expensive, but it does not take into account small distortions of bond lengths and angles introduced by the steric encumbrance of the *tert*-butyl groups. In Table 3, some selected coordinates are compared for the two geometries. It appears that only very small differences can be found, among which the most noticeable is the lengthening of the N2−C3 distance in diradical **1b**, caused, by the repulsion between the bridge and the *tert*-butyl groups. Since ΔE_{ST} is an observable very sensitive to the chemical details of the bridge, it could be of some interest to investigate if the (very small) increase of the magnetic site−bridge distance contributes

dx.doi.org/10.1021/ct100602y |*J. Chem. Theory Comput.* 2011, 7, 699–706

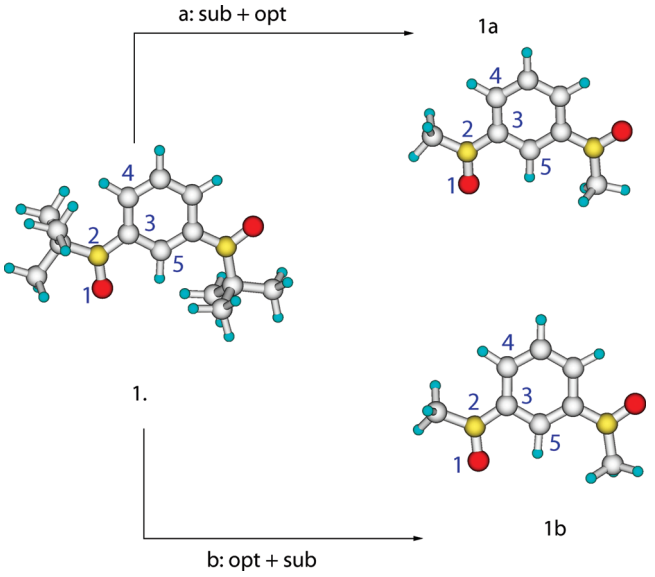

Figure 3. Two different routes to obtain a model of diradical **1** (see Figure 2 suitable for DDCI calculations. (a) *tert*-Butyl groups are first substituted with methyls (sub), and thereafter a full optimization (opt) is performed. (b) The substitution is performed on the optimized geometry of the whole diradical.

Table 3. Selected Internal Coordinates for the Two Optimized Geometries of Model Diradicals 1a and 1b[a]

coordinate	1a	1b
O1−N2	1.276 Å	1.278 Å
N2−C3	1.407 Å	1.423 Å
C3−C4	1.409 Å	1.410 Å
O1−C5	2.721 Å	2.637 Å
O1−N2−C3	120.6°	117.6°
N2−C3−C4	121.6°	124.6°
N2−C4−C5	118.0°	116.0°
O1−N2−C3−C4	180.0°	180.0°

[a] Atom numbers refer to Figure 3.

to diminishing the interaction between the magnetic sites. Furthermore, the capability of the proposed procedure to meet chemical intuition and reproduce such small effects could be considered a further proof of the protocol reliability.

Singlet−triplet energy gaps were computed combining MVO and CSPA approaches, for the whole diradical **1** and the smaller model in the two geometries **1a** and **1b**. All results are reported in Table 4, together with the variational space dimensions (VSD) and the CPU time employed, and in Figure 4, as a function of the ratio (Var %) between the MVO active to the variational treatment in the CSPA approach (VAVO), and the total number of MVOs.

The calculations performed on the whole diradical were not able to consider a DDCI variational space larger than 30% of that subtended by all VOs, due to the excessive requests of both memory and CPU time. However, it seems from the left panel of Figure 4 that the reported values are near to converge around a value of ∼290 cm^{-1}. As far as the two smaller models are concerned, it is evident that neglecting the small differences between geometries **1a** and **1b** does have some consequence on the final estimate of ΔE_{ST}, the former being larger (326 cm^{-1}) than the one expected for the whole original molecule. Conversely, if the geometrical effects of the presence of the *tert*-butyl groups are taken into account by adopting the b model route (see Figure 3), the results obtained are very close (286.1 cm^{-1}) to those found for the whole diradical **1**. It also appears from Table 4 that the CPU time savings amply offsets the computational burden of optimization route b. Furthermore, it is worth stressing that the adoption of the CSPA approximation allows us to handle such calculations at a reasonable computational cost, exploiting the improved convergence rate of the CSPA corrected results. Indeed, by looking at the right panel of Figure 4, where the full variational limit is reported for the model compound (in **1b** geometry), one can see that only about 30% of the MVO can be treated at a variational level, without losing much accuracy in the estimate of the final results. This allows for a savings of almost a factor 20 on CPU time. It may be worth stressing that the full variational limit, obtained with a VAVO/MVO ratio of 100%, is exactly the same value that could be obtained by employing all canonical virtual orbitals in a completely variational calculation, as reported in the orginal paper where MVOs were first proposed.[58]

Finally, our computational results can be compared with experimental estimates reported for the whole diradical **1**. Notwithstanding, **1** is not fully persistent in solution (it isomerizes into an aminiquinone imine N-oxide in a few hours). The dependence of its magnetic susceptivity χ from the temperature was measured, and an estimate of $\Delta E_{ST} > 300$ K (210 cm^{-1}) was given by the authors,[17] in fair agreement with the present theoretical findings (∼420 K).

3.2. 4,6-Trifluoromethyl, *m*-Phenylene Bis(*tert*-butyl)-nitroxide. Substitution of the of two hydrogens at positions 4 and 6 in the phenylene bridge with two trifluoromethyl groups leads to the formation of diradical **2** (see Figure 2). In this case, the modeling route based on replacing each *tert*-butyl group on the N atoms with a methyl moiety must be handled with care, since its effects on the minimum geometry are expected to be remarkably larger than those found in the previous case, due to the steric interaction between the *tert*-butyl groups and the trifluoromethyl substituents of the bridge. In fact, as can be seen from Figure 5, where the computed torsional energy surfaces are reported for *tert*-butyl and the methyl nitroxides, it appears that the presence of the larger substituent on N atoms dramatically alters the PES profile, resulting in a nonplanar minimum geometry, with the dihedral angles Φ_1 and Φ_2 placed at 65° and 125°, respectively. The dependence of the singlet−triplet gap in aromatic bridged nitroxides from such torsional dihedrals is well-known, both experimentally[18,21,67,68] and theoretically.[30,57] In particular it has been found that distortions from planarity in *meta* substituted aromatic bridges sensibly diminishes the stability of the triplet state, eventually leading[68] in some cases to a more stable singlet, i.e., yielding antiferromagnetic behavior. For this reason, the modeling route b, discussed in the previous section (see Figure 3), has been followed also in this case, substituting with hydrogen atoms the methyl groups of the *tert*-butyl moieties in the minimum energy nonplanar geometry, found for the whole diradical **2** (see panel a of Figure 5).

The three-step procedure has been applied on this latter configuration. First, MOs have been localized onto three fragments, namely, the *m*-phenylene bis(methyl)-nitroxide and the two trifluoromethyls. Subsequently, the MVO+CSPA scheme has been employed only on those MOs localized on the former moiety, whereas those MOs pertaining to the CF_3 fragments are discarded. The resulting ΔE_{ST}'s are reported in Table 5. By

Table 4. ΔE_{ST} Computed with the MVO/CSPA DDCI Scheme for the Whole Diradical 1 and for the Two Geometries of the Smaller Model Di-Nitroxide[a]

	target diradical (**1**)			model diradicals (**1a** and **1b**)			
Var (%)	VSD (10^3 det.)	CPU time	ΔE_{ST} (cm^{-1})	VSD (10^3 det.)	CPU time	ΔE_{ST}^{1a} (cm^{-1})	ΔE_{ST}^{1b} (cm^{-1})
10	573	2 days, 12 h	316.1	133	3 h	262.7	231.8
15	907	7 days, 13 h	311.9	267	12 h	332.8	295.5
25	1755	15 days, 7 h	300.3	439	23 h	322.6	287.4
30	2844	20 days, 12 h	296.2	648	1 day, 12 h	319.8	286.3
35				894	2 days, 1 h	318.2	284.7
40				1500	3 days, 13 h	318.5	284.6
50				1726	4 days, 13 h	318.7	284.9
55				2254	5 days, 15 h	323.0	285.2
100				5417	17 days, 12 h	326.5	286.1

[a] The ratio VAVO/MVO is reported in the first column (Var %), while the dimensions of the DDCI space treated variationally (VSD, expressed in number of configurations) appears in the second column.

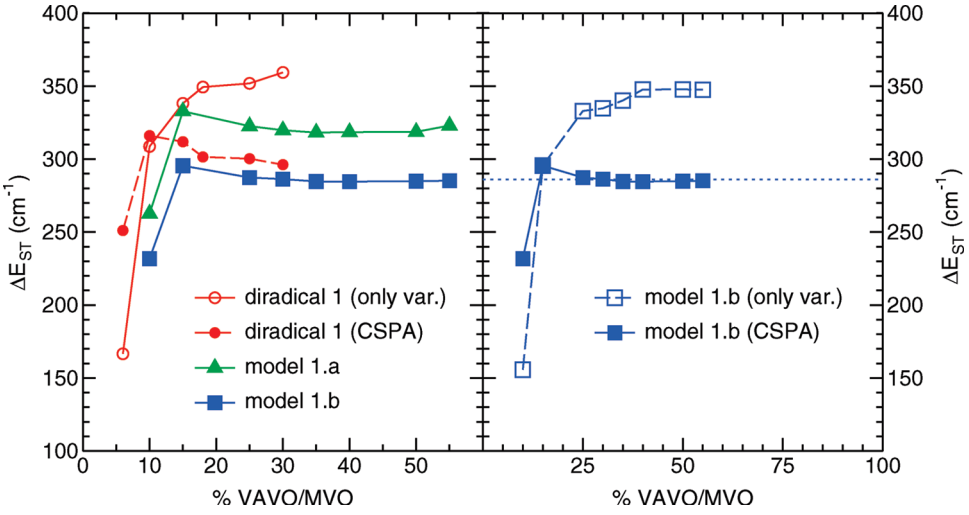

Figure 4. ΔE_{ST} as a function of the VAVO/MVO ratio. Left panel: Singlet−triplet energy gaps are compared for the whole (**1**, red symbols) and the model diradicals (**1a** and **1b**). For the larger compound, results obtained without the CSPA correction are also reported with empty red circles. Right panel: Convergence of the CSPA uncorrected (empty triangles) and corrected (full triangles) approach is compared for geometry **1b** of the model compound. The dotted line is the result of a complete variational treatment.

looking at these results, it appears that the singlet−triplet interaction is reduced by an order of magnitude with respect to diradical **1**, due to the substitution of the trifluoromethyl moieties, whose major effect is to displace outside the plane containing the aromatic ring the oxygen atoms bearing the unpaired electrons. This remarkable reduction is also in agreement with the experimental findings. In fact, despite an unexpected antiferromagnetic behavior being experimentally registered[21] at room temperature, the triplet state was found to be the most stable at very low temperatures, where the minimum energy conformer is expected to be more populated. In these conditions, a best fit estimate of 80 K (∼55 cm^{-1}) was reported[21] for ΔE_{ST}, i.e., well below the lower limit value of 300 K given[17] for its parent homologue **1**. It is also worth pointing out that, thanks to CSPA, the computed value is nearly converged by treating variationally only less than 20% of all MVOs, thus allowing a remarkable savings of computational time.

3.3. Biphenyl-3,5-diyl Bis(*tert*-butyl Nitroxide). Diradical **3** is obtained from diradical **1** by substitution of a hydrogen atom, placed in position 5 on the phenylene bridge, with a phenyl ring (see Figure 2). As in previous cases, modeling route b has been followed; i.e., the whole diradical has been first optimized, and thereafter the methyl groups of the *tert*-butyl-nitroxides were substituted with hydrogen atoms. Differently from compound **2**, this diradical retains a planar structure of the *m*-phenylene bis-nitroxide moiety; that is, the oxygen atoms are coplanar to the bridge aromatic ring. Conversely, the phenyl substituent in position 5 is found at ∼40° with respect to the bridge, so that a negligible conjugation between the two rings is expected. The latter observation allows us to apply the fragmentation procedure, projecting out from the DDCI configurational space all MOs localized onto the substituent phenyl ring. Computed ΔE_{ST} as a function of the VAVO/MVO ratio is reported in Figure 6. As in previous cases, convergence around a value of ∼300 cm^{-1} is reached rather quickly, and a reliable estimate of the magnetic energy gap can be obtained by applying a variational approach to only 20−25% of the total number of MVOs, leaving the remaining VOs for the perturbative correction of the CSPA.

The value obtained is again in agreement with experimental estimates. Indeed, notwithstanding the first measures[19] performed on the α phase of diradical **3** crystal unexpectedly revealing a

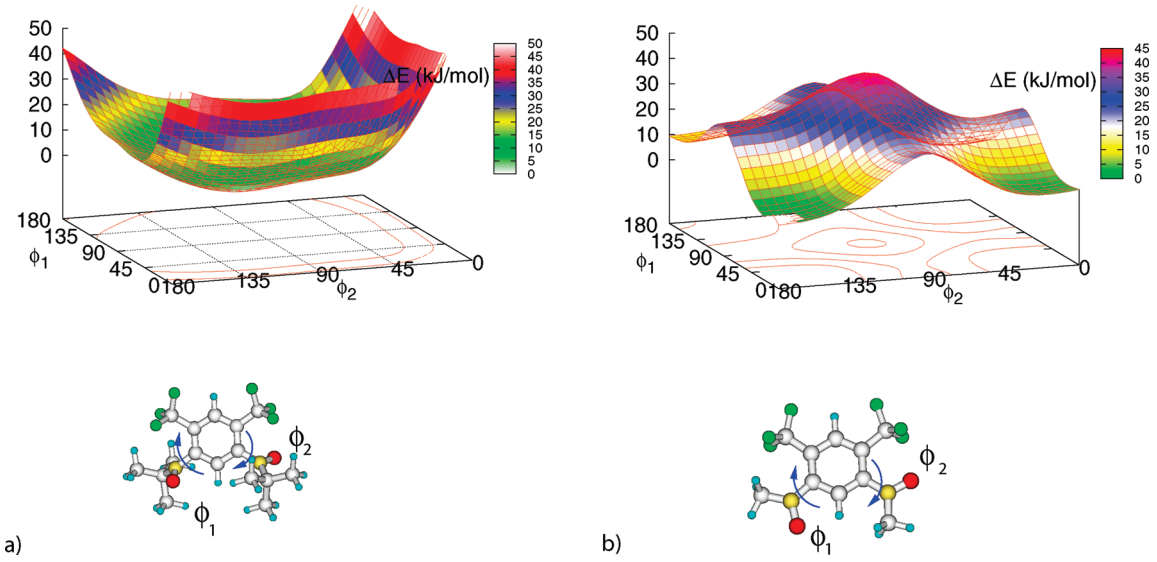

Figure 5. Torsional potential energy profiles for 4,6-trifluoromethyl, *m*-phenylene bis(*tert*-butyl)-nitroxide diradical **2** (panel a) and the 4,6-trifluoromethyl, *m*-phenylene bis(methyl)-nitroxide diradical (panel b). Dihedrals Φ_1 and Φ_2 are indicated with blue arrows.

Table 5. ΔE_{ST} Computed with the Three-Step DDCI Scheme for Diradical 2

VAVO/MVO (%)	detors	CPU time	ΔE_{ST} (cm^{-1})
10	114676	5 h	21.9
15	239296	17 h	26.7
25	400116	1 days, 6 h	26.6
30	597136	1 days, 21 h	26.5
35	830356	2 days, 9 h	26.4
45	1099776	3 days, 3 h	26.3
50	1405396	3 days, 19 h	26.5
55	1747216	4 days, 22 h	26.5
65	1747216	5 days, 14 h	26.9

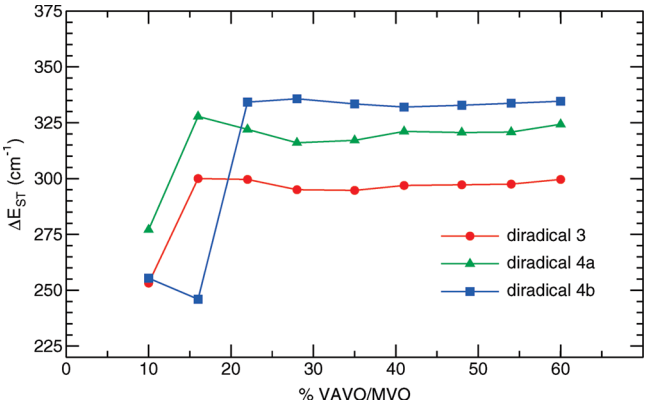

Figure 6. Singlet−triplet splittings ΔE_{ST} as a function of the VAVO/MVO ratio, computed for diradical **3** (circles) and two different models of diradical **4** (triangles and squares for a and b, respectively).

diamagnetic nature, further investigations[20] proved the existence of a second (β) crystal phase, in which the triplet state was shown to be the most stable. In particular, the antiferromagnetic response of the crystal in the α phase was attributed to intermolecular interactions between nitroxides of neighboring molecules, while an intramolecular origin was inferred for phase β. In the latter case, both crystallographic data (bridge-nitroxides planarity and 40.2° intraring torsion[20]) and the best fit estimate of the singlet−triplet gap (ΔE_{ST} > 350 K) are in agreement with our computed data (39.5° and 431 K).

3.4. Pegylated Bis(aminoxyl) Diradical. The dimensions of diradical **4** compelled us to choose a simpler model to represent the polymeric substituent. Despite the effect on ΔE_{ST} of both the reciprocal orientation between the polymeric and magnetic bearing moieties and the conformational mobility of the polyethylene glycol substituent needing to be taken into account, the aim of the present work is to test the sensitivity of the proposed computational protocol to different substituents. For this reason, only two models, in their fully optimized geometry, will be taken into account for the calculation of the singlet−triplet energy splitting of diradical **4**. Besides the substitution of the *tert*-butyl groups (which was again performed according to the aforementioned modeling route b), the polymeric chain was represented by two alkoxyl substituents, namely $(CH_3O)(CH_3)_2C-$ (diradical **4a**) and $(CH_3O)(CH_3)(CH_3CH_2OCH_2)C-$ (diradical **4b**), whose minimum energy conformations are shown respectively in panels a and b of Figure 7. The two geometries are identical in their *m*-phenylene moiety, whereas some differences can be spotted in the relative orientation of the aliphatic substituents with respect to the bridge. Indeed, in compound **4a**, the oxygen of the methoxyl group lies in the same plane as the aromatic ring, causing the two methyls to be in symmetric position with respect to the bridge. Conversely, in model **4b**, the methoxyl group is out-of-plane by ∼12°, and the polymeric fragment is nearly perpendicular to the ring plane.

For both models, the same fragmentation scheme has been applied, retaining for the DDCI calculations only those MOs localized in the nitroxides+bridge moiety. Computed singlet−triplet magnetic splittings are reported in Figure 6 as a function of the VAVO/MVO ratio. ΔE_{ST}'s are in both cases greater than the one computed for diradical **3**, with model **4b** showing a slightly larger value (≃ 490 K) than model **4a** (≃ 470 K). The agreement with the experimental data[16] is less satisfactory than for the first three diradicals studied, even if the best fit estimate of ∼650 K

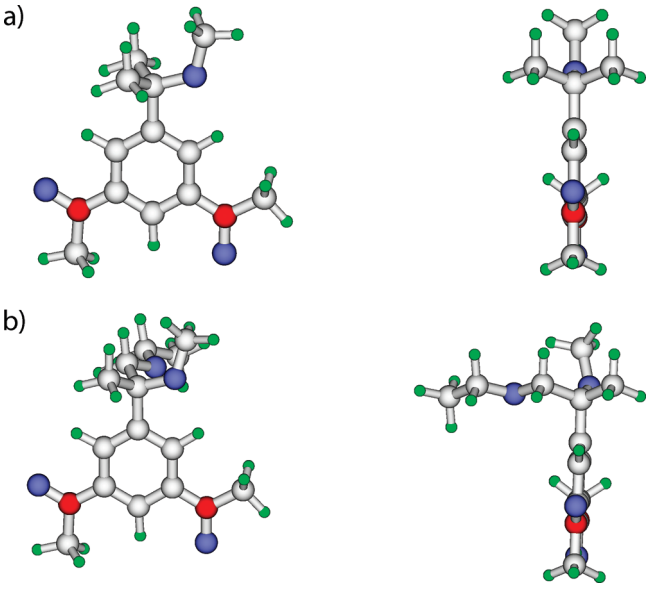

Figure 7. Front and side views of model diradicals **4a** and **4b** in their optimized geometries.

given by Rajca and co-workers could be somewhat overestimated (see note 17 in ref 16). However, it should be pointed out that, besides not considering the whole polymer chain, the present calculations do not include any dynamical effect, due to conformational mobility and/or interaction with the solvent, that could affect the ΔE_{ST} value.

4. CONCLUSIONS

A new integrated strategy for an accurate calculation of singlet−triplet magnetic splittings has been tested and validated. The procedure essentially consists of three steps, where the MVO and CSPA approaches, recently proposed by our group,[58,59] are now combined on a DDCI configurational space previously reduced by fragmentation/localization criteria. This approach has been tested successfully on four different substituted *m*-phenylene bis(*tert*butyl) nitroxides, which are experimentally known to possess a stable triplet state.

The fragmentation schemes sensibly reduce the DDCI space dimensions but still allow evaluation of the effect of different substituents, as they are able to distinguish between very similar models (e.g., model **4a** and **4b**). From a computational point of view, the application of the CSPA scheme allowed us to remarkably reduce the dimensions of the variationally treated space without a sensible loss in the accuracy of the calculations. More important, the optimal VAVO/MVO ratio (25−30%) seems not to depend on the diradical under study and could be confidently applied to larger systems. On the other hand, if *a priori*, "chemical" models (e.g., the substitution of the *tert*-butyl groups with smaller methyl moieties) are to be adopted, attention must be paid to the effect that such changes can introduce to the target diradical geometry, as ΔE_{ST} was shown to be rather sensitive to even small geometrical changes involving the bridge connecting the two magnetic moieties.

Finally, considering the difficulties in the experimental estimate of such a quantity, and the uncertainty that it is known[1,18,22,24] to affect the best fit procedure, the proposed computational route could be considered as a powerful auxiliary technique for the accurate determination of magnetic interactions.

AUTHOR INFORMATION

Corresponding Author

*E-mail: giacomo.prampolini@sns.it.

REFERENCES

(1) Rajca, A. *Chem. Rev.* **1994**, *94*, 871.
(2) Rajca, A.; Wongsriratanakul, J.; Rajca, S. *Science* **2001**, *294*, 1503.
(3) Kahn, O. *Molecular Magnetism*; VCH Publishers Inc.: New York, 1993; p 393.
(4) Coronado, E.; Delhaès, P.; Gatteschi, D.; Milles, J. S. *Molecular Magnetism: From Molecular Assemblies to the Devices*; Kluwer Academic Publishers: Dordrecht, The Netherlands, 1996; NATO ASI Series Vol. E321.
(5) Gatteschi, D.; Sessoli, R.; Villain, J. *Molecular nanomagnets*; Oxford University Press: Oxford, U. K., 2006.
(6) Rajca, A.; Wongsriratanakul, J.; Rajca, S. *J. Am. Chem. Soc.* **2004**, *126*, 6608.
(7) Fukuzaki, E.; Nishide, H. *J. Am. Chem. Soc.* **2006**, *128*, 996.
(8) Matsuda, K.; Iwamura, H. *Curr. Opin. Solid State Mater. Sci.* **1997**, *2* (4), 446–450.
(9) Koivisto, B. D.; Hicks, R. G. *Coord. Chem. Rev.* **2005**, *249*, 2612–2630.
(10) Murata, H.; Miyajima, D.; Nishide, H. *Macromolecules* **2006**, *39*, 6331–6335.
(11) Itoh, T.; Hirai, K.; Tornioka, H. *Bull. Chem. Soc. Jpn.* **2007**, *80*, 138–157.
(12) Nishimaki, H.; Ishida, T. *J. Am. Chem. Soc.* **2006**, *132*, 9598.
(13) Zhdanov, R. *Bioactive Spin Labels*; Springer-Verlag: Berlin, 1992.
(14) Marx, L.; Rassat, A. *Chem. Commun.* **2002**, 632.
(15) Francese, G.; Dunand, F.; Loosli, C.; Merbach, A.; Decurtins, S. *Magn. Reson. Chem.* **2003**, *43*, 81.
(16) Spagnol, G.; Shiraishi, K.; Rajca, S.; Rajca, A. *Chem. Commun.* **2005**, 5047.
(17) Ishida, T.; Iwamura, H. *J. Am. Chem. Soc.* **1991**, *113*, 4238.
(18) Dvolaitzky, M.; Chiarelli, R.; Rassat, A. *Angew. Chem., Int. Ed.* **1992**, *31*, 180.
(19) Kurokawa, G.; Ishida, T.; Nogami, T. *Chem. Phys. Lett.* **2004**, *392*, 74.
(20) Nishimaki, H.; Mashiyama, S.; Yasui, M.; Nogami, T.; Ishida, T. *Chem. Mater.* **2006**, *18*, 3602.
(21) Rajca, A.; Lu, K.; Rajca, S.; Ross, C., II. *Chem. Commun.* **1999**, 1249.
(22) Rajca, A.; Shiraishi, K.; Rajca, S. *Chem. Commun.* **2009**, 4372.
(23) Rajca, A.; Vale, M.; Rajca, S. *J. Am. Chem. Soc.* **2008**, *130*, 9099.
(24) Rajca, A.; Shiramishi, K.; Pink, M.; Rajca, S. *J. Am. Chem. Soc.* **2007**, *129*, 7232.
(25) Noodleman, L.; Norman, J. G. *J. Chem. Phys.* **1979**, *70*, 4903.
(26) Noodleman, L. *J. Chem. Phys.* **1981**, *74*, 5737.
(27) Barone, V.; Bencini, A.; Ciofini, I.; Daul, C. A. *J. Phys. Chem. A* **1999**, *103*, 4275.
(28) Adamo, C.; Barone, V.; Bencini, A.; Totti, F.; Ciofini, I. *Inorg. Chem.* **1999**, *38*, 1996.
(29) Ali, M. E.; Datta, S. N. *J. Phys. Chem. A* **2006**, *110*, 2776.
(30) Ali, M. E.; Roy, A. S.; Datta, S. N. *J. Phys. Chem. A* **2007**, *111*, 5523.
(31) Illas, F.; Moreira, I. de P. R.; Bofill, J. M.; Filatov, M. *Theor. Chem. Acc.* **2006**, *116*, 587.
(32) Rivero, P.; Moreira, I. de P. R.; Illas, F.; Scuseria, G. E. *J. Chem. Phys.* **2008**, *129*, 184110.
(33) Bencini, A. *Inorg. Chim. Acta* **2008**, *361*, 3820.
(34) Moreira., I. de P. R.; Illas, F. *Phys. Chem. Chem. Phys.* **2006**, *8*, 1645.
(35) Bencini, A.; Totti, F. *J. Chem. Theory Comput.* **2009**, *5*, 144.
(36) de Loth, P.; Cassoux, P.; Daudey, J. P.; Malrieu, J. P. *J. Am. Chem. Soc.* **1981**, *103*, 4007.

(37) Miralles, J.; Daudey, J. P.; Caballol, R. *Chem. Phys. Lett.* **1992**, *198*, 555.
(38) Miralles, J.; Castell, O.; Caballol, R.; Malrieu, J. P. *Chem. Phys.* **1993**, *172*, 33.
(39) Castell, O.; Caballol, R.; Subra, R.; Grand, A. *J. Phys. Chem.* **1995**, *99*, 154.
(40) de Graaf, C.; Sousa, C.; Moreira., I. de P. R.; Illas, F. *J. Phys. Chem. A* **2001**, *105*, 11371.
(41) Angeli, C.; Calzado, C. J.; Cimiraglia, R.; Evangelisti, S.; Guihéry, N.; Leininger, T.; Malrieu, J.-P.; Maynau, D.; Ruitz, J. V. P.; Sparta, M. *Mol. Phys.* **2003**, *101*, 1389.
(42) Calzado, C. J.; Cabrero, J.; Malrieu, J. P.; Caballol, R. *J. Chem. Phys.* **2002**, *116*, 2728.
(43) Calzado, C. J.; Cabrero, J.; Malrieu, J. P.; Caballol, R. *J. Chem. Phys.* **2002**, *116*, 3985.
(44) Cabrero, J.; Ben Amor, N.; de Graaf, C.; Illas, F.; Caballol, R. *J. Phys. Chem. A* **2000**, *104*, 9983.
(45) Neese, F. *J. Chem. Phys.* **2003**, *119*, 9428.
(46) Calzado, C. J.; Angeli, C.; Taratiel, D.; Caballol, R.; Malrieu, J.-P. *J. Chem. Phys.* **2009**, *131*, 044327.
(47) de Graaf, C.; Caballol, R.; Romo, S.; Poblet, J. M. *Theor. Chem. Acc.* **2009**, *123*, 3.
(48) Calzado, C. J.; Angeli, C.; Caballol, R.; Malrieu, J.-P. *Theor. Chem. Acc.* **2010**, *126*, 185.
(49) Monari, A.; Maynau, D.; Malrieu, J.-P. *J. Chem. Phys.* **2010**, *133*, 44106.
(50) Queralt, N.; Taratiel, D.; de Graaf, C.; Caballol, R.; Cimiraglia, R.; Angeli, C. *J. Comput. Chem.* **2008**, *29*, 994.
(51) Rota, J.-B.; Norel, L.; Train, C.; Ben Amor, N.; Maynau, D.; Robert, V. *J. Am. Chem. Soc.* **2008**, *130*, 10380.
(52) Bastardis, R.; Guihery, N.; de Graaf, C. *J. Chem. Phys.* **2008**, *129*, 104102.
(53) Maurice, R.; Guihery, N.; Bastardis, R.; de Graaf, C. *J. Chem. Theory Comput.* **2010**, *6*, 55.
(54) Calzado, C. J.; Angeli, C.; de Graaf, C.; Caballol, R. *Theor. Chim. Acc.* **2010**, DOI:10.1007/s00214-010-0831-6.
(55) Barone, V.; Cacelli, I.; Ferretti, A.; Girlanda, M. *J. Chem. Phys.* **2008**, *128*, 174303.
(56) Barone, V.; Cacelli, I.; Ferretti, A. *J. Chem. Phys.* **2009**, *130*, 94306.
(57) Barone, V.; Cacelli, I.; Cimino, P.; Ferretti, A.; Monti, S.; Prampolini, G. *J. Phys. Chem. A* **2009**, *113*, 15150.
(58) Barone, V.; Cacelli, I.; Ferretti, A.; Prampolini, G. *Phys. Chem. Chem .Phys* **2009**, *11*, 3854.
(59) Barone, V.; Cacelli, I.; Ferretti, A.; Prampolini, G. *J. Chem. Phys.* **2009**, *131*, 224103.
(60) Barone, V.; Cacelli, I.; Ferretti, A.; Prampolini, G. *Phys. Chem. Chem. Phys.* **2010**under revision.
(61) Pipek, J.; Mezey, P. G. *J. Chem. Phys.* **1989**, *90*, 4916.
(62) Frisch, M. J.; Trucks, G. W.; Schlegel, H. B.; Scuseria, G. E.; Robb, M. A.; Cheeseman, J. R.; Montgomery, J. A., Jr.; Vreven, T.; Kudin, K. N.; Burant, J. C.; Millam, J. M.; Iyengar, S. S.; Tomasi, J.; Barone, V.; Mennucci, B.; Cossi, M.; Scalmani, G.; Rega, N.; Petersson, G. A.; Nakatsuji, H.; Hada, M.; Ehara, M.; Toyota, K.; Fukuda, R.; Hasegawa, J.; Ishida, M.; Nakajima, T.; Honda, Y.; Kitao, O.; Nakai, H.; Klene, M.; Li, X.; Knox, J. E.; Hratchian, H. P.; Cross, J. B.; Bakken, V.; Adamo, C.; Jaramillo, J.; Gomperts, R.; Stratmann, R. E.; Yazyev, O.; Austin, A. J.; Cammi, R.; Pomelli, C.; Ochterski, J. W.; Ayala, P. Y.; Morokuma, K.; Voth, G. A.; Salvador, P.; Dannenberg, J. J.; Zakrzewski, V. G.; Dapprich, S.; Daniels, A. D.; Strain, M. C.; Farkas, O.; Malick, D. K.; Rabuck, A. D.; Raghavachari, K.; Foresman, J. B.; Ortiz, J. V.; Cui, Q.; Baboul, A. G.; Clifford, S.; Cioslowski, J.; Stefanov, B. B.; Liu, G.; Liashenko, A.; Piskorz, P.; Komaromi, I.; Martin, R. L.; Fox, D. J.; Keith, T.; Al-Laham, M. A.; Peng, C. Y.; Nanayakkara, A.; Challacombe, M.; Gill, P. M. W.; Johnson, B.; Chen, W.; Wong, M. W.; Gonzalez, C.; Pople, J. A. *Gaussian 03*, Revision C.02; Gaussian, Inc.: Wallingford, CT, 2004.
(63) Schmidt, M. W.; Baldridge, K. K.; Boats, J. A.; Elbert, S. T.; Gordon, M. S.; Jensen, J. H.; Koseki, S.; Matsunaga, N.; Nguyen, K. A.; Su, S. J.; Windus, T. L.; Dupuis, M.; Montgomery, J. A. *J. Comput. Chem.* **1993**, *14*, 1347.
(64) Huron, B.; Malrieu, J. P.; Rancurel, P. *J. Chem. Phys.* **1973**, *58*, 5745.
(65) Evangelisti, S.; Daudey, J. P.; Malrieu, J. P. *Chem. Phys.* **1983**, *75*, 91.
(66) Cimiraglia, R.; Persico, M. *J. Comput. Chem.* **1987**, *8*, 39.
(67) Shultz, D.; Boal, A.; Lee, H.; Farmer, G. *J. Org. Chem.* **1999**, *64*, 4386.
(68) Shultz, D.; Fico, R.; Kampf, H. L. J.; Kirschbaum, K.; Pinkerton, A.; Boyle, P. *J. Am. Chem. Soc.* **2003**, *125*, 15426.